

RESEARCH ARTICLE

Biochemical Characterization of Three BLT Receptors in Zebrafish

Toshiaki Okuno^{1,2*}, Tohru Ishitani³, Takehiko Yokomizo^{1,2}

1 Department of Biochemistry, Juntendo University School of Medicine, Tokyo, Japan, **2** Department of Medical Biochemistry, Kyushu University, Fukuoka, Japan, **3** Division of Cell Regulation Systems, Department of Immunobiology and Neuroscience, Medical Institute of Bioregulation, Kyushu University, Fukuoka, Japan

* tokuno@juntendo.ac.jp



OPEN ACCESS

Citation: Okuno T, Ishitani T, Yokomizo T (2015) Biochemical Characterization of Three BLT Receptors in Zebrafish. PLoS ONE 10(3): e0117888. doi:10.1371/journal.pone.0117888

Academic Editor: Roland Seifert, Medical School of Hannover, GERMANY

Received: November 12, 2014

Accepted: January 5, 2015

Published: March 4, 2015

Copyright: © 2015 Okuno et al. This is an open access article distributed under the terms of the [Creative Commons Attribution License](https://creativecommons.org/licenses/by/4.0/), which permits unrestricted use, distribution, and reproduction in any medium, provided the original author and source are credited.

Data Availability Statement: The sequence of zebrafish Blt1 is available from EMBL/GenBank/DDBJ under accession no. LC009449. The sequences of zebrafish Blt2 are available from EMBL/GenBank/DDBJ under accession nos. LC009450 and LC009451.

Funding: This work was supported by Grants-in-Aid for Scientific Research from the Ministry of Education, Culture, Sports, Science, and Technology of Japan (nos. 21390083, 22116001, and 22116002 to T.Y.; and nos. 25460374 and 24102522 to T.O.), the Naito Foundation, the Ono Medical Research Foundation, the Uehara Memorial Foundation, the Takeda Science Foundation, and the Inamori Foundation.

Abstract

The leukotriene B₄ (LTB₄) receptor 1 (BLT1) is a high affinity receptor for LTB₄, a chemotactic and inflammatory eicosanoid. The LTB₄ receptor 2 (BLT2) was originally identified as a low affinity receptor for LTB₄, and, more recently, as a high affinity receptor for 12-hydroxyheptadecatrienoic acid (12-HHT). The zebrafish BLT receptors have not been previously identified and the *in vivo* functions of these receptors have been unknown. In this paper, we describe one zebrafish BLT1-like receptor, Blt1, and two zebrafish BLT2-like receptors, Blt2a and Blt2b. Cells expressing Blt1 exhibited LTB₄-induced intracellular [Ca²⁺] increases, inhibition of cAMP production, ligand-dependent [³⁵S]GTPγS binding, and transforming growth factor-α (TGFα) shedding activity in a dose-dependent manner, similar to human BLT1. Cells expressing Blt2a and Blt2b exhibited 12-HHT- and LTB₄-induced intracellular [Ca²⁺] increases, inhibition of cAMP production, [³⁵S]GTPγS binding, and TGFα shedding activity, with a dose-dependency similar to human BLT2. Reverse transcription (RT)-PCR analysis and whole-mount *in situ* hybridization revealed that *blt1*, *blt2a*, *blt2b*, zebrafish LTA₄ hydrolase (*lta4h*), and zebrafish 5-lipoxygenase (*5lo*) are expressed in zebrafish embryos. Knockdown of *blt1* by morpholino antisense oligonucleotides resulted in delayed epiboly at gastrulation. Consistently, knockdown of *lta4h*, an enzyme mediating LTB₄ production, induced a phenotype similar to knockdown of *blt1*. These results suggest that the LTB₄-BLT1 axis is involved in epiboly in zebrafish development.

Introduction

Leukotriene B₄ (LTB₄), an eicosanoid derivative of arachidonic acid metabolism produced by the sequential actions of 5-lipoxygenase (5-LO) and leukotriene A₄ hydrolase (LTA₄H), is a potent leukocyte chemoattractant [1]. Two G-protein-coupled receptors (GPCRs) for LTB₄, BLT1 and BLT2, have been identified [2]. BLT1 is a high affinity LTB₄ receptor [3], while BLT2 was originally identified as a low affinity LTB₄ receptor [4]. Recently, we demonstrated that 12(S)-hydroxy-5-cis-8,10-trans-heptadecatrienoic acid (12-HHT), which had been considered as merely a by-product of thromboxane synthesis from prostaglandin endoperoxide, is an

The funders had no role in study design, data collection and analysis, decision to publish, or preparation of the manuscript.

Competing Interests: The authors have declared that no competing interests exist.

endogenous high affinity ligand for BLT2 [5,6]. BLT1 and BLT2 form a gene cluster on both human and mouse chromosomes, suggesting that these receptors were generated by a gene duplication machinery [4]. BLT1 is expressed on various immune cells including neutrophils, eosinophils [7], monocytes, dendritic cells [8,9], activated T-cells [10], and osteoclasts [11], and induces the activation and migration of these cells [12]. The *in vivo* role of BLT2 has not been established, but our recent work revealed that BLT2 has an anti-inflammatory function in a mouse model of inflammatory colitis [13], as well as a protective role in allergic airway inflammation [14]. BLT2 also promotes wound healing by accelerating keratinocyte migration [15].

The zebrafish has emerged as a useful model system for genetic and pharmacological analyses of embryogenesis because fertilization and embryo development occur outside the maternal body and the embryos are transparent [16,17]. In addition, the zebrafish has been used as a model for studying inflammation and immunity because the immune system is largely conserved between zebrafish and mammals. Bichel *et al.* have shown that LTB₄ induces neutrophil migration into the fins of live zebrafish [18], and recent forward genetic screening in zebrafish larvae has revealed that the *lta4h* locus modulates susceptibility to mycobacterial infections [19,20]. However, BLT receptors have not been definitively identified in zebrafish. In this study, we identified genes for zebrafish BLT receptors by bioinformatic and biochemical analyses, and revealed an unexpected function of zebrafish BLT1 in embryogenesis.

Material and Methods

Materials

LTB₄ and 12-HHT were purchased from Cayman Chemical (Ann Arbor, MI). Probenecid was purchased from Sigma-Aldrich (St. Louis, MO). Pluronic F-127, Alexa-488-conjugated anti-Rat IgG (Molecular Probes), and fetal calf serum (FCS; GIBCO) were obtained from Invitrogen (Carlsbad, CA). A penicillin-streptomycin solution and geneticin (G418) were purchased from Nacalai Tesque (Kyoto, Japan). [³⁵S]-guanosine 5'-O-(gamma-thio) triphosphate (GTPγS) was obtained from Perkin-Elmer Life Science (Boston, MA). Anti-hemagglutinin (anti-HA; clone 3F10) was purchased from Roche (Penzberg, Germany).

cDNA cloning and plasmid construction of zebrafish Blts

The cDNA of zebrafish *blt1*, *blt2a*, *blt2b* and *lta4h* were isolated by PCR from cDNA templates prepared from zebrafish embryos at 24–72 hours post fertilization (hpf). The following primers were used for cDNA cloning: *blt1* (5'- atggcaactccttaactccggtc -3' and 5'-tcaatgcaggggggtcagagtcttg -3'), *blt2a* (5'- atggcgttgaaccttctgtccccc -3' and 5'-tcaattccattattctgggggtgcg -3'), *blt2b* (5'-atggcattggaaaatggcagcttctc -3' and 5'-ttatagcctgatgacatccctagtc-3'), and *lta4h* (5'-atgac tccagtttcagaccctagc-3' and 5'-ctagccatcgattttcagatccttg-3'). The sequences for *blt1*, *blt2a* and *blt2b* were amplified by PCR and cloned into the pCXN2-HA vector [21]. The following primers were used: *blt1*, (5'- ttgcgatatcgcaactccttaactccggcttctc -3' and 5'-gccaattctcaatgcaggggggtcagagtc -3'), *blt2a* (5'- ttgcgatatcgcttgaaccttctgtccccc -3' and 5'-gccaattctcactttcattattctgggggtgc-3'), and *blt2b* (5'-ttgcgatatcgattggaaaatggcagcttctc-3' and 5'-gccaattctatagcctgatgac atccctag- 3'). Zebrafish *blt1*, *blt2a*, and *blt2b* were amplified by PCR and cloned into the pCS2+ vector. Zebrafish *lta4h* and *5lo* were amplified by PCR and cloned into the pCS2P+ vector. The following primers were used: *lta4h* (5'-cggaattccaccatgactcagatttcagaccctagc-3' and 5'-ccgctcagctagccatcgattttcagatccttg-3') and *5lo* (5'-cggaattcgttggaaaatgcccagctacacgg-3' and 5'-ccgctcagctagctacacagccactgttggattc-3'). All of the clones were verified by DNA sequencing.

Cell culture, transfection, and cell sorting

Chinese hamster ovary (CHO) cells were maintained in Ham's F-12 medium (Wako) containing 10% FCS, 100 units/ml penicillin, and 100 µg/ml streptomycin in 5% CO₂ at 37°C. CHO cells were transfected with expression vectors using Lipofectamine LTX and the PLUS Reagent (Invitrogen) according to the manufacturer's protocol. At 48 h post-transfection, the medium was changed to selection medium containing 1 mg/ml G418. After 2–3 weeks of selection, G418-resistant cells were stained with anti-HA (2 µg/ml) and Alexa-Fluor 488-conjugated anti-Rat IgG (10 µg/ml). Cells expressing the BLT receptors were collected as polyclonal populations by cell sorting using FACSAria II (Becton, Dickinson and Company, Franklin Lakes, NJ) and maintained in 0.3 mg/ml G418. A FACSCalibur instrument (Becton Dickinson) was used for flow cytometry.

Calcium mobilization assay

CHO cells (3×10^4) stably expressing one of the receptors were seeded onto 96-well plates. After 16 h, cells were loaded with 4 µM Fluo-8 AM (ABD Bioquest) in 100 µl of HP buffer (HBSS containing 2.5 mM probenecid and 20 mM HEPES, pH 7.4) supplemented with 0.04% Pluronic F-127 and 1% FCS at 37°C for 30 min, followed by a further incubation at room temperature for 30 min. The cells were washed twice with HP buffer and agonist-induced intracellular calcium mobilization was determined by monitoring the fluorescence intensity (excitation at 485 nm, emission at 525 nm) using a FlexStation 3 plate reader (Molecular Devices, Sunnyvale, CA).

Membrane preparation and GTPγS binding assay

Cells were harvested and sonicated in ice-cold homogenization buffer (20 mM Tris-HCl, pH 7.4, 0.25 M sucrose, 10 mM MgCl₂, and 2 mM EDTA) containing a protease inhibitor mixture (Nacalai Tesque, Kyoto Japan). The homogenate was centrifuged at 800 × g for 5 min at 4°C; the supernatant was collected and centrifuged at 100,000 × g for 1 h at 4°C. The resulting pellet was resuspended in the homogenization buffer. The membrane preparation (10 µg of protein) was incubated in 100 µl of GTPγS binding buffer (20 mM Tris-HCl, pH 7.5, 100 mM NaCl, 5 mM MgCl₂, 1 mM EDTA, 1 mM DTT, 5 µM GDP and 0.1% BSA) containing 1 nM [³⁵S]GTPγS with LTB₄ or 12-HHT for 30 min at 30°C. To determine nonspecific binding, unlabeled GTPγS was added to the binding mixture to a final concentration of 10 µM. The bound [³⁵S]GTPγS was separated from free [³⁵S]GTPγS by rapid filtration through GF/C filters and washed with ~2 ml of ice-cold TMN buffer (10 mM Tris-HCl, pH 7.5, 25 mM MgCl₂, and 100 mM NaCl). The radioactivity of the filters was determined using a Top Count scintillation counter (Packard Instrument Co.).

cAMP assay

CHO cells (4×10^4 cells/well) were plated on 96-well plates. On the following day, cells were washed twice with Krebs-Ringer Bicarbonate Buffer containing glucose (KRBG buffer: 0.49 mM MgCl₂, 4.56 mM KCl, 120 mM NaCl, 0.7 mM Na₂HPO₄, 1.5 mM NaHPO₄, 15 mM NaHCO₃ and 10 mM glucose (pH 7.4)). The cells were incubated with stimulation buffer (KRBG buffer containing 0.75 mM 3-isobutyl-1-methylxanthine (IBMX)) for 10 min at room temperature and then with 20 µM forskolin and LTB₄, or 12-HHT, for 15 min at 37°C. The incubation was terminated by the addition of lysis buffer (pH 7.3) supplied in the CatchPoint cAMP Fluorescent Assay Kit (Molecular Devices Corporation), and the concentration of cAMP in the lysate was determined according to the manufacturer's protocol.

TGF α shedding assay

A TGF α shedding assay was performed as previously reported [22]. HEK cells (2×10^5 cells/well) were seeded into 12-well plates and incubated for 24 h. The cells were then transfected with the GPCR expression vector, pCAGGS-G $\alpha_{q/i1}$ and pSS-AP-TGF α . At 24 h post-transfection, the cells were detached and resuspended in Hank's balanced salt solution (HBSS) containing 5 mM HEPES (pH 7.4) and then seeded in a 96-well plate. After a 30 min incubation for 37°C, cells were stimulated with ligand for 1 h. The conditioned medium was transferred into another 96-well plate and *p*-nitrophenyl phosphate (*p*-NPP) solution (10 mM *p*-NPP, 40 mM Tris-HCl (pH 9.5), 40 mM NaCl and 10 mM MgCl₂) was added to both a conditioned medium plate and a cell plate. Absorbance at 405 nm (OD₄₀₅) of both plates was read before and after a 1 h incubation at 37°C using a microplate reader (Bio-rad). To determine TGF α shedding, AP activity was calculated from the increase in OD₄₀₅ in the conditioned medium ($\Delta OD_{\text{medium}}$) relative to the cell plate (ΔOD_{cell}) as follows. AP activity in the conditioned medium (AP_{media}) (%) was defined as the ratio of $\Delta OD_{\text{medium}}$ to total ΔOD values ($\Delta OD_{\text{medium}}$ plus ΔOD_{cell}).

Zebrafish maintenance, morpholino injection and RT-PCR

Zebrafish strain AB was maintained under standard conditions. All experimental animal care was performed in accordance with institutional and national guidelines and regulations. The study protocol was approved by the institutional review board of Kyushu University. (All the experiments were performed at Kyushu University). Morpholino antisense oligonucleotides (MO) were designed and obtained from Gene Tools (Philomath, OR, USA). The sequences of translation-blocking MO and splice-blocking MO against *blt1* were 5'—GGCCATTTGACTCAAACCTTTATGGT- 3' (*blt1* MO) and 5'—CTATTAGACATACCGATAAAAATGGC—3' (*blt1* spl MO), respectively. The translation-blocking MO against *lta4h* (*lta4h* MO) has been described previously [19]. To test the specificities of the *Blt1* MO and *lta4h* MO, the MO target sequences of *Blt1* and *lta4h* were amplified by PCR and cloned into the pCS2P-EGFP vector (kindly provided by A. Kawahara, University of Yamanashi). MOs (5 ng) were injected into zebrafish embryos at the one- or two-cell stage. Total RNA from control MO- or *blt1* spl MO-injected embryos was obtained at 24 hpf using the Trizol reagent (Invitrogen-Gibco, Carlsbad, CA) and was used as the template for generating cDNA (Superscript II reverse transcriptase; Invitrogen-Gibco). A 338 base pair (bp) *blt1* fragment was amplified using the following primers: *blt1_fw*, 5'—aggctgaggaccaagaagaggctcc—3', and *blt1_rv*, 5'—ggcaaccagaagagggtgaaagcag—3'. The 392 bp nonsplicing transcript of *blt1* was amplified using the following primers: *blt1_fw* and *blt1_rv2* 5'—aatgctggtgccgctctattgat—3'. A 264 bp *blt2a* fragment was amplified using the following primers: *blt2a_fw*, 5'—tgggactttctgcaccgttttagc—3', and *blt2a_rv*, 5'—gtccgaaggtgacgacaatcaccag—3'. A 299 bp *blt2b* fragment was amplified using the following primers: *blt2b_fw*, 5'—gcgtctgtactgcagactgaccgt—3', and *blt2b_rv*, 5'—ggcttgaatgaggttctgcttctg—3'. A 251 bp *lta4h* fragment was amplified using the following primers: *lta4h_fw*, 5'—gctcttctctcgtctccaagt—3', and *lta4h_rv*, 5'—aaggcagggtgattccaaagggg—3'. A 330 bp *5lo* fragment was amplified using the following primers: *5lo_fw*, 5'—tgaaaatgccagc-tacacggtgac—3', and *5lo_rv*, 5'—ctttgcatcaaccaaccagcggaag—3'.

Whole-mount *in situ* hybridization

Whole-mount *in situ* hybridization was performed according to a standard protocol. A digoxigenin-labeled antisense RNA probe was prepared using pCS2-*blt1*, pCS2-*blt2a*, pCS2-*blt2b*, and pCS2-*lta4h*. Capped mRNA was synthesized using an SP6 mMessage mMachine kit (Ambion, Austin, TX, USA) and purified using Micro Bio-Spin columns (Bio-Rad, Hercules, CA, USA).

Statistical Analysis

Statistical analysis was performed using Prism (Graphpad Software) for all comparisons.

Results

Cloning of *blt1* and *blt2* homologs in zebrafish

To obtain cDNAs for BLT receptors in zebrafish, we searched for putative zebrafish BLT receptors and identified three BLT-like sequences (XP_002662767, XP_009301152, XP_003197923) from the NCBI database. We amplified full-length cDNAs corresponding to these three sequences and cloned each into an expression vector. From the results of the pharmacological experiments described below, XP_002662767, XP_009301152, and XP_003197923 were named *blt1*, *blt2a*, and *blt2b*, respectively. We aligned the amino acid sequences of zebrafish, human, and mouse BLT1 (Fig. 1), and found that they shared moderate homology, with sequence identities of 38% between zebrafish and human or mouse. We also aligned the amino acid sequences of zebrafish, human and mouse BLT2 (Fig. 2), and found that they shared relatively low homology with sequence identities of 29–34% between zebrafish and human or mouse (Fig. 3A). A phylogenetic analysis showed that zebrafish BLTs form a clade independent from mammalian BLT1 and BLT2 (Fig. 3B). In human and mouse, the *blt1* and *blt2* genes are located on chromosome 14. In zebrafish, the *blt1* and *blt2a* genes are located on chromosome 7, and the *blt2b* gene is located on chromosome 2 (Fig. 3C).

Ligand identification and intracellular signaling of Blt1, Blt2a, and Blt2b

To examine the ligands and intracellular signaling of zebrafish Blt1, Blt2a, and Blt2b, we established CHO cells stably expressing N-terminally HA-tagged zebrafish Blt1, Blt2a, and Blt2b, as well as human BLT1 (hBLT1) and BLT2 (hBLT2). CHO cells expressing the receptors were sorted as polyclonal populations and analyzed using a flow cytometer. The hBLT1 and zebrafish Blt1 were expressed on the cell surface at similar levels (Fig. 4A), and hBLT2, zebrafish Blt2a, and Blt2b were expressed on the cell surface at similar levels (Fig. 4B). Previously, we showed that human BLT1 and BLT2 are coupled to the Gi and Gq families of G-proteins [23–25]. To investigate intracellular signaling through zebrafish BLTs, we performed calcium mobilization assays using the transfected cells. In hBLT1 (Fig. 5B) and zebrafish Blt1 (Fig. 5C) cells, intracellular free calcium concentration increased in a dose-dependent manner in response to LTB₄ stimulation, whereas 12-HHT did not induce calcium mobilization in these cells, suggesting that zebrafish Blt1 is a zebrafish ortholog of human BLT1. In hBLT2 (Fig. 5D), zebrafish Blt2a (Fig. 5E), and zebrafish Blt2b (Fig. 5F) cells, the intracellular free calcium exhibited a dose-dependent increase in response to either 12-HHT or LTB₄ stimulation, and 12-HHT activated zebrafish Blt2a and Blt2b at lower doses than LTB₄, suggesting that zebrafish Blt2a and Blt2b are zebrafish orthologs of hBLT2.

Next, we quantified cAMP levels in CHO cells expressing the receptors. In hBLT1 (Fig. 6B) and zebrafish Blt1 (Fig. 6C) cells, 10 nM LTB₄ inhibited forskolin-induced cAMP formation, but 12-HHT did not, suggesting that zebrafish Blt1 is a high affinity LTB₄ receptor similar to hBLT1. In hBLT2 (Fig. 6D), zebrafish Blt2a (Fig. 6E), and zebrafish Blt2b (Fig. 6F) cells, 10 nM 12-HHT inhibited cAMP formation, but LTB₄ had only a minimal effect on cAMP, suggesting that zebrafish Blt2a and Blt2b are high affinity 12-HHT receptors similar to hBLT2. To confirm that zebrafish BLT receptors directly activated G-proteins, we performed GTPγS binding assays using a membrane preparation of CHO cells expressing the receptors. Incubation with 1 μM LTB₄ induced robust GTPγS binding, but 12-HHT did not, in hBLT1 (Fig. 7B) and zebrafish Blt1 (Fig. 7C) cells. Incubation with 1 μM 12-HHT induced robust GTPγS binding, and

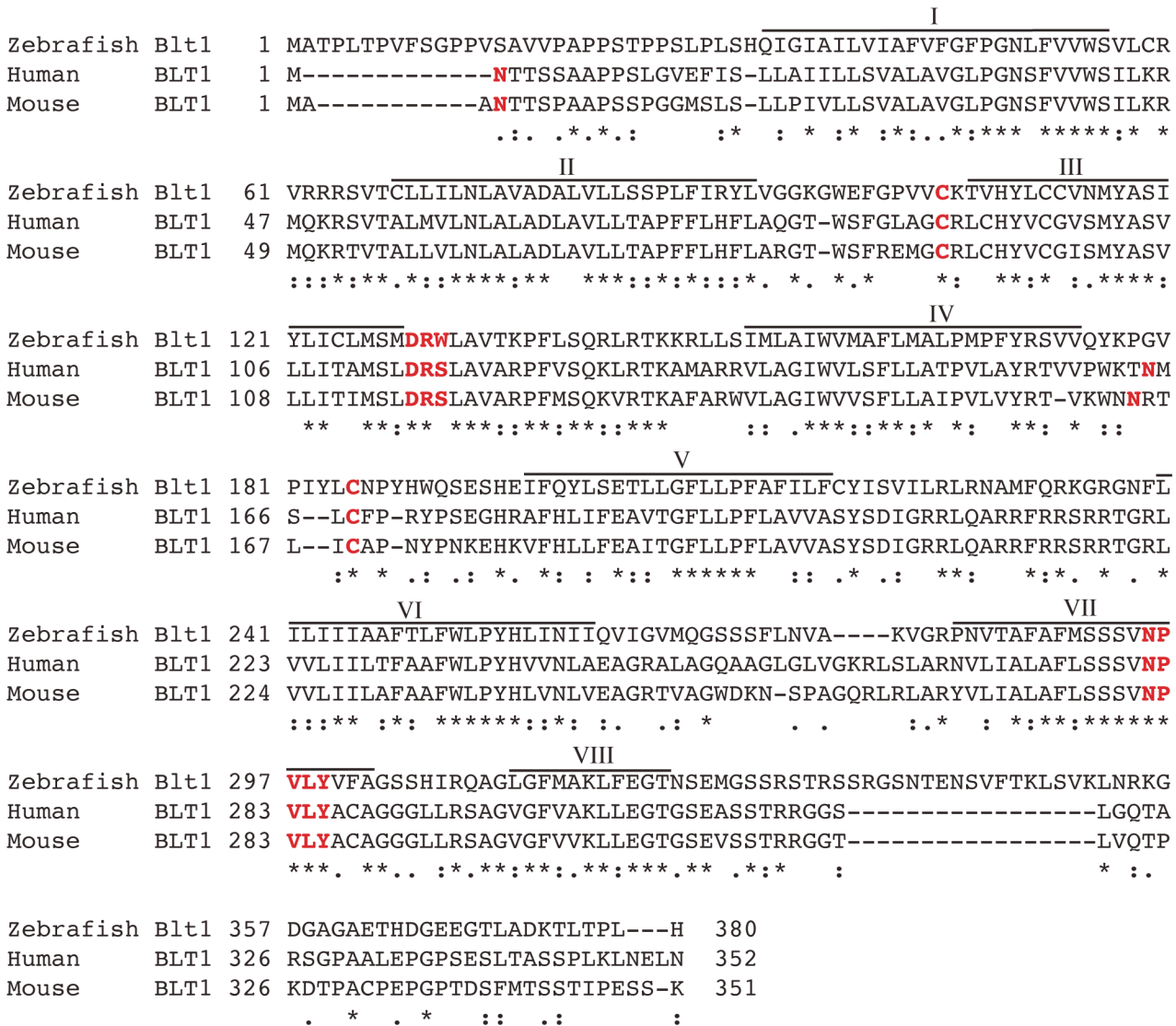


Fig 1. Sequence alignment of zebrafish Blt1 with human and mouse BLT1. The amino acid sequences of zebrafish Blt1 and human and mouse BLT1 were aligned using MAFFT (<http://www.ebi.ac.uk/Tools/msa/mafft/>). Identical residues are indicated with asterisks (*), highly conserved residues with colons (:), and semi-conserved residues with periods (.). The predicted glycosylated aspartate, the predicted cysteine residues that form disulfide bonds, and the DRW and N/DPxxY motifs are indicated in red characters. Putative helical domains that form helix I to helix VIII are indicated above the aligned sequences. The sequence of zebrafish Blt1 is available from EMBL/GenBank/DDBJ under accession no. LC009449.

doi:10.1371/journal.pone.0117888.g001

1 μ M LTB₄ induced moderate but significant GTP γ S binding, in hBLT2 (Fig. 7D), zebrafish Blt2a (Fig. 7E), and zebrafish Blt2b (Fig. 7F) cells. These results suggest that zebrafish Blt1 is a BLT1-type receptor, and zebrafish Blt2a and Blt2b are BLT2-type receptors.

TGF α shedding activities of zebrafish Blt1, Blt2a, and Blt2b

To confirm the ligands and intracellular signaling of zebrafish BLT receptors, we performed a TGF α shedding assay. In the TGF α shedding assay, GPCR activation is measured by the ecto-domain shedding of a membrane-bound pre-form of alkaline phosphatase-tagged TGF α (AP-TGF α) into the medium [22]. HEK293 cells were transfected with a GPCR expression vector, a G_{q/11} chimeric plasmid, and an expression plasmid encoding AP-TGF α , and then

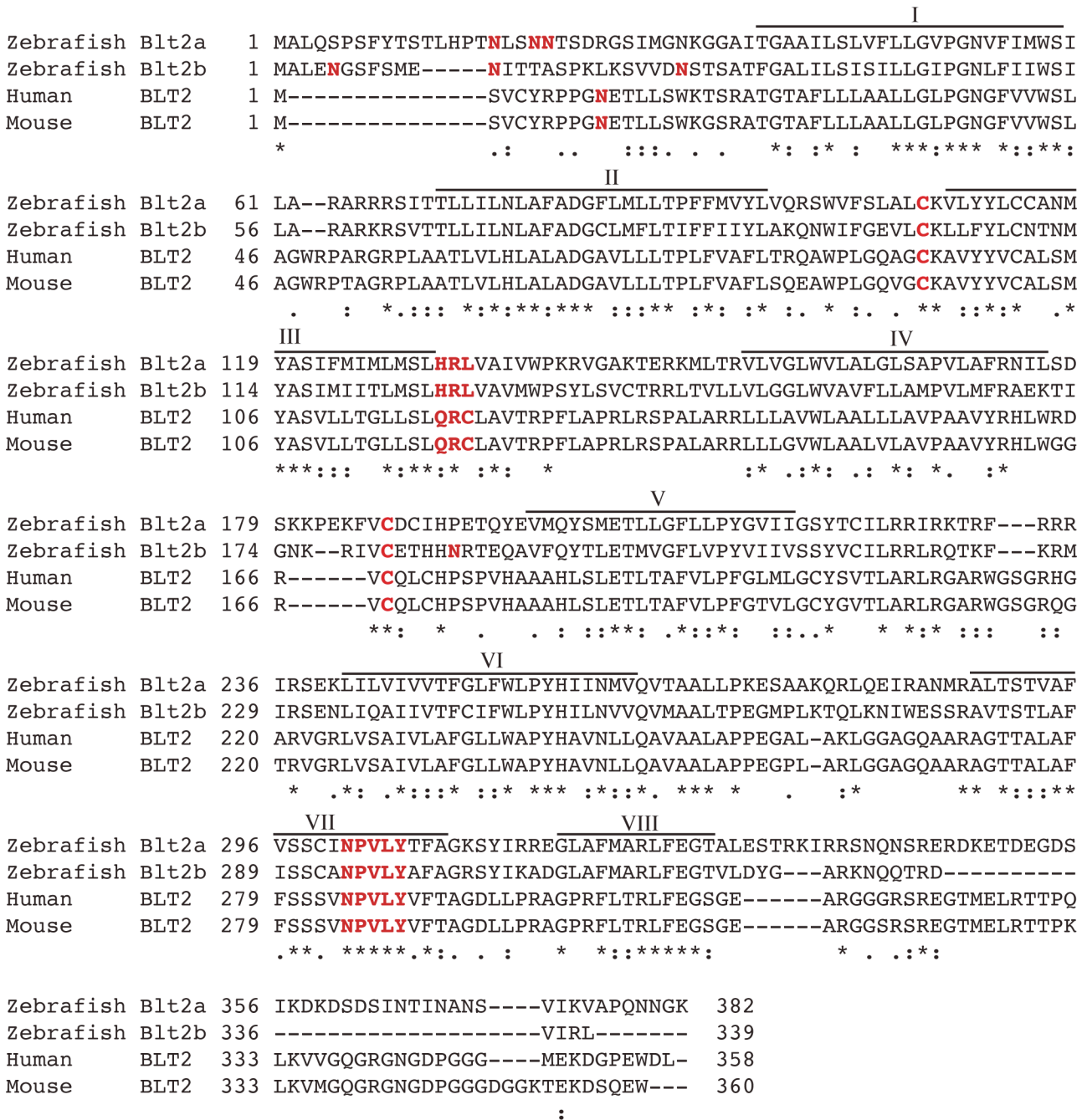


Fig 2. Sequence alignment of zebrafish Blt2a and Blt2b with human and mouse BLT2. The amino acid sequences of zebrafish Blt2 and human and mouse BLT2 were aligned using MAFFT (<http://www.ebi.ac.uk/Tools/msa/mafft>). Identical residues are indicated with asterisks (*), highly conserved residues with colons, and semi-conserved residues with periods (.). The predicted glycosylated aspartate, the predicted cysteine residues that form disulfide bonds, and the DRY and N/DPxxY motifs are indicated in red. Putative helical domains that form helix I to helix VIII are indicated above the aligned sequences. The sequences of zebrafish Blt2 are available from EMBL/GenBank/DBJ under accession nos. LC009450 and LC009451.

doi:10.1371/journal.pone.0117888.g002

stimulated with a ligand, which resulted in the accumulation of released AP-TGF α into the medium (conditioned medium). LTB $_4$ stimulation resulted in a dose-dependent increase in TGF α shedding that was similar between hBLT1 (Fig. 8A) and zebrafish Blt1 (Fig. 8B) cells. In hBLT2 (Fig. 8C), zebrafish Blt2a (Fig. 8D), and Blt2b (Fig. 8E) cells, TGF α shedding activity was

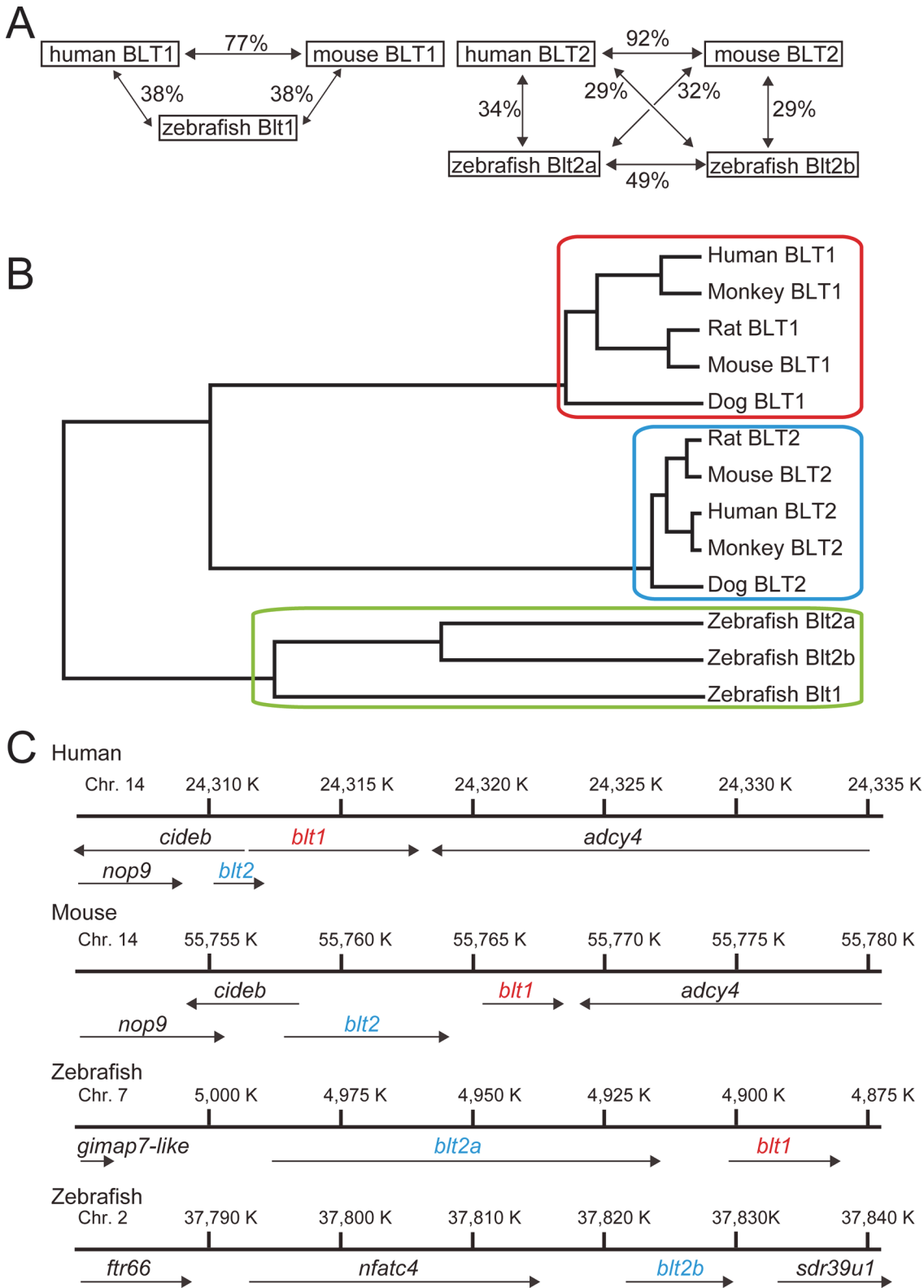


Fig 3. Sequence analysis of the zebrafish Blt receptors. (A) The amino acid identities among BLT1s (left) and BLT2s (right) are illustrated. (B) A phylogenetic tree of BLT homologs in chordates was generated by GENETEX-MAC using the Unweighted Pair Group Method using the arithmetic Average (UPGMA). (C) Chromosomal locations of the human, mouse, and zebrafish *blt1* and *blt2* genes are shown. Chr., chromosome; *cideb*, cell death-inducing dffa-like effector b; *nop9*, nucleolar protein; *adc4*, adenylate cyclase 4; *gimap7-like*, GTPase IMAP family member 7-like; *ftr66*, fin TRIM family, member 66; *nfatc4*, nuclear factor of activated T-cells, cytoplasmic, calcineurin-dependent 4; *sdr39u1*, short chain dehydrogenase/reductase family 39U.

doi:10.1371/journal.pone.0117888.g003

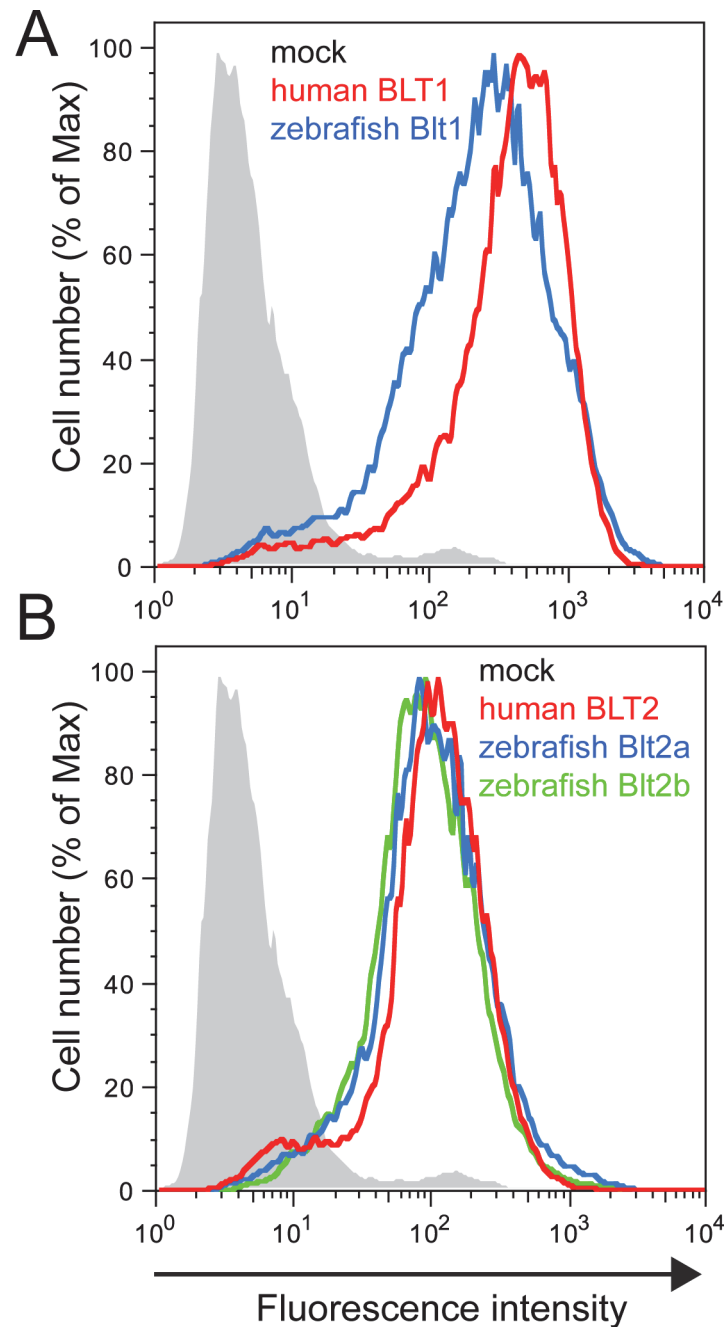


Fig 4. Establishment of CHO cells expressing the zebrafish Blt receptors. CHO cells stably expressing hBLT1, zebrafish Blt1, hBLT2, zebrafish Blt2a, or Blt2b were sorted after staining the cell surface Blts using an anti-HA antibody, and the surface expression was analyzed by flow cytometry.

doi:10.1371/journal.pone.0117888.g004

dose-dependently increased by either 12-HHT or LTB₄ stimulation. The lower AP activity of zebrafish Blt2a (Fig. 8D) may be affected by the lower expression of Blt2a on the cell surface in this assay (data not shown). In zebrafish Blt2b cells (Fig. 8E), the TGF α shedding activity induced by LTB₄ was much lower than that induced by 12-HHT. Thus, Blt2b may exhibit greater specificity for 12-HHT than that shown by hBLT2.

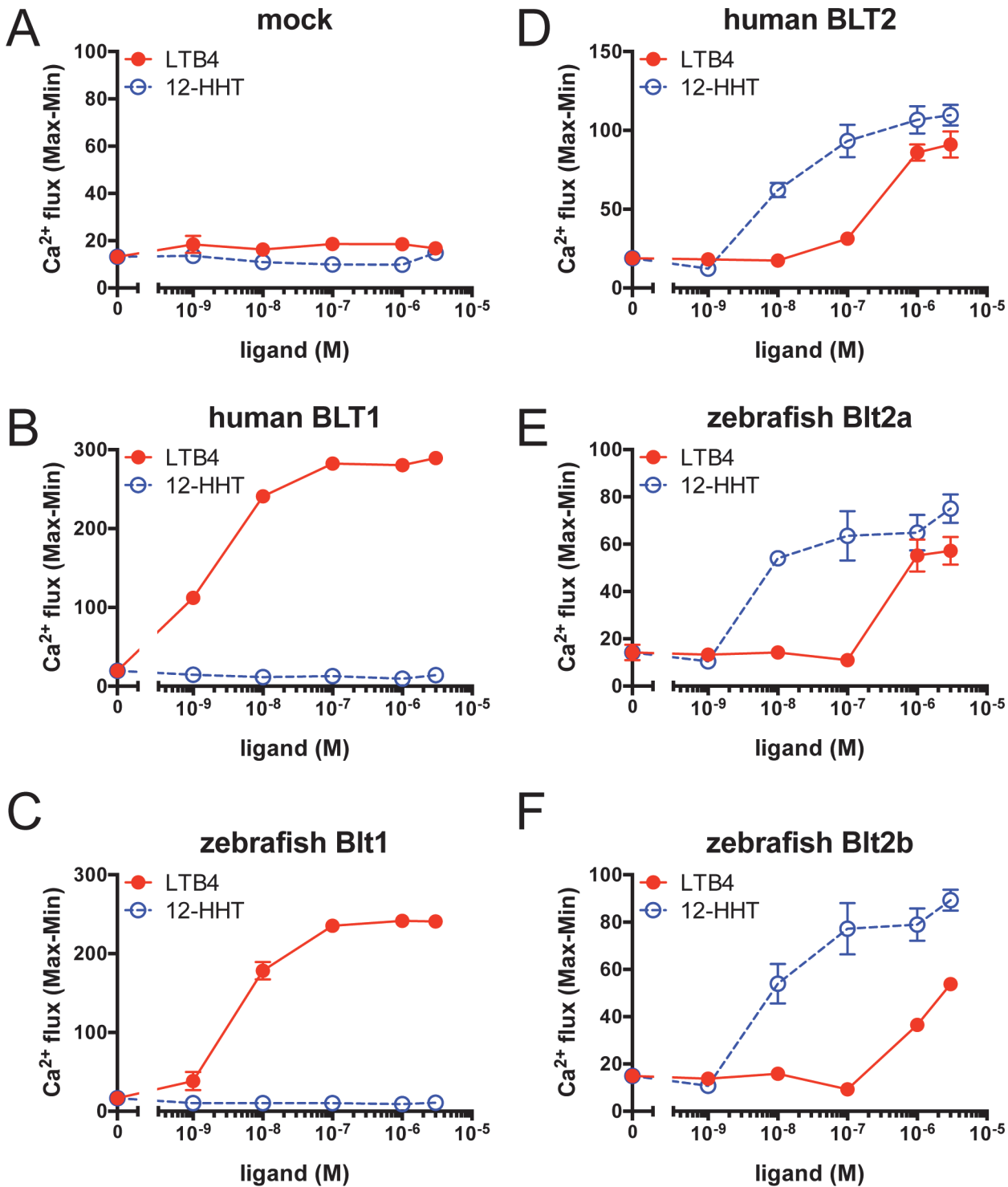


Fig 5. Calcium mobilization in CHO cells expressing the zebrafish Blt receptors. Intracellular calcium mobilization in CHO cells stably expressing hBLT1, zebrafish Blt1, hBLT2, zebrafish Blt2a, or Blt2b was analyzed using a FlexStation plate reader to measure fluorescence intensity. Data represent the mean \pm s.e.m. (n = 4). These data are representative of at least two independent experiments with similar results.

doi:10.1371/journal.pone.0117888.g005

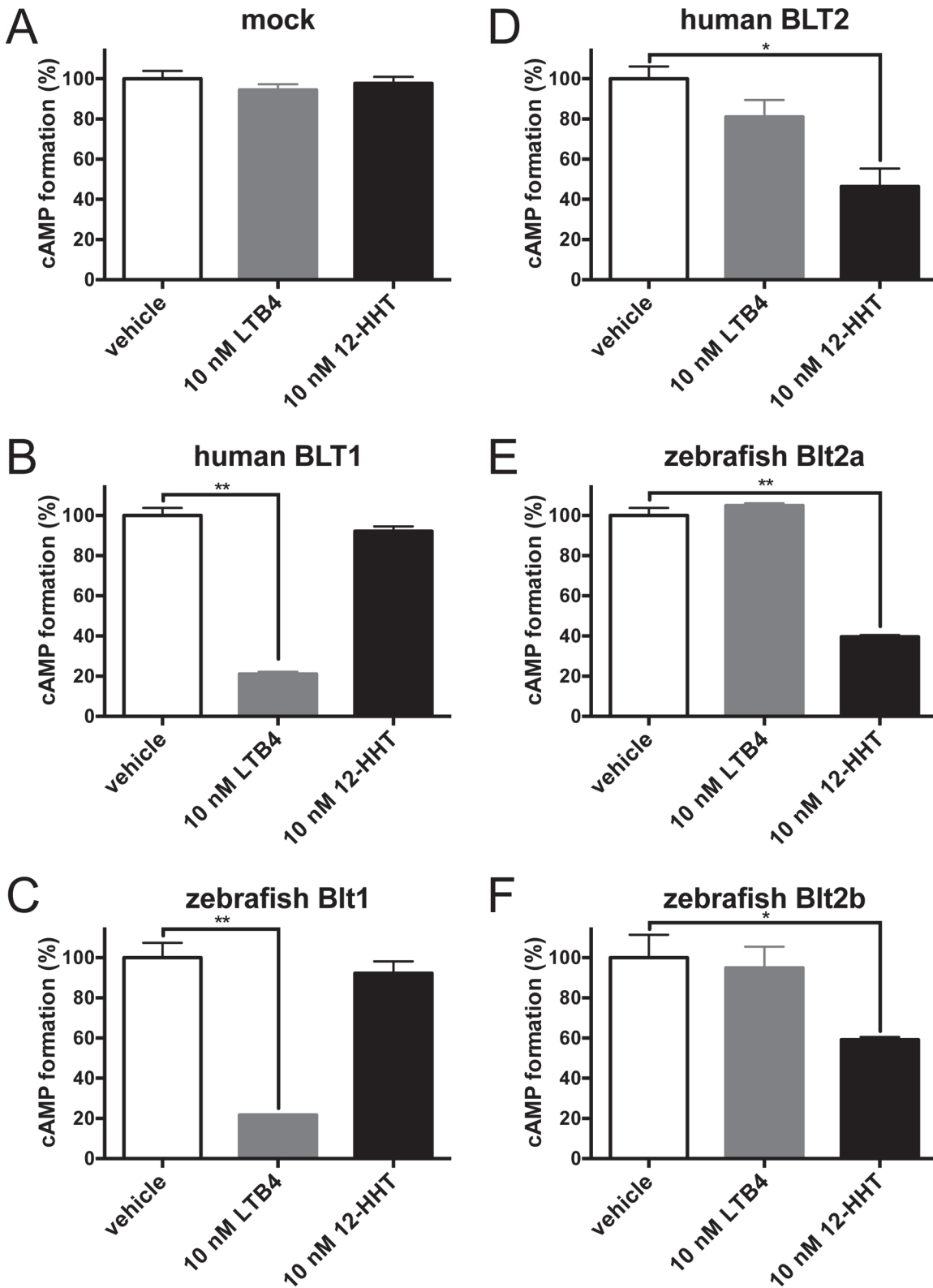


Fig 6. Levels of cAMP in CHO cells expressing the zebrafish BLT receptors. CHO cells stably expressing the human or zebrafish receptors were stimulated with 20 μ M forskolin and 10 nM LTB₄ or 12-HHT, and the levels of cAMP in cell lysates were determined. Data represent the mean \pm s.e.m. (n = 3). **, P < 0.005; *, P < 0.05, one-way ANOVA with Bonferroni post-hoc test. These data are representative of at least two independent experiments with similar results.

doi:10.1371/journal.pone.0117888.g006

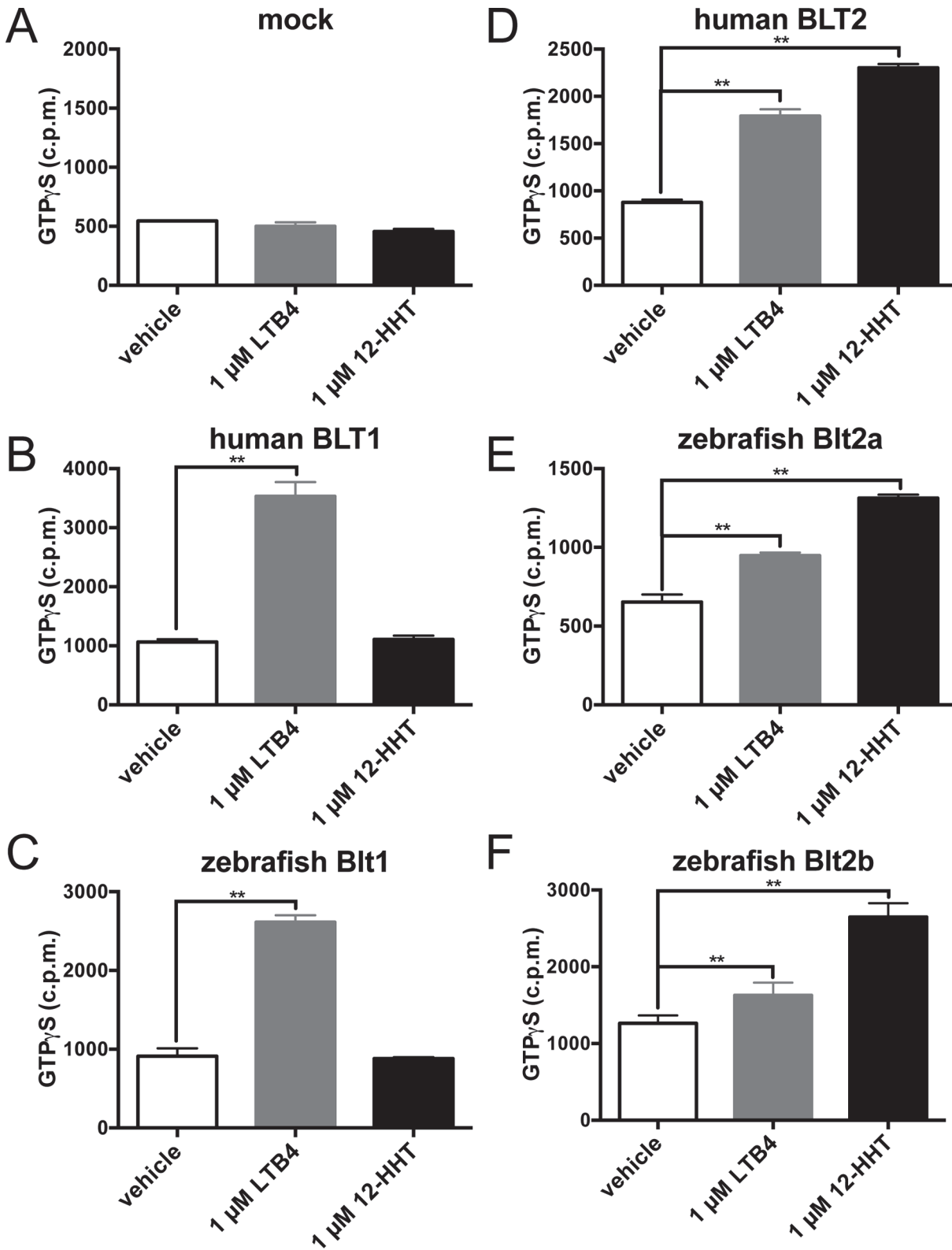


Fig 7. G-protein activity in CHO cells expressing the zebrafish Blt receptors. Membrane preparations of CHO cells expressing human or zebrafish receptors were incubated with 1 nM [³⁵S] GTP γ S and 1 μ M LTB₄ or 12-HHT, and specific binding was measured. Data represent the mean \pm s.e.m. (n = 3). **, P < 0.005, one-way ANOVA with Bonferroni post-hoc test. These data are representative of at least two independent experiments with similar results.

doi:10.1371/journal.pone.0117888.g007

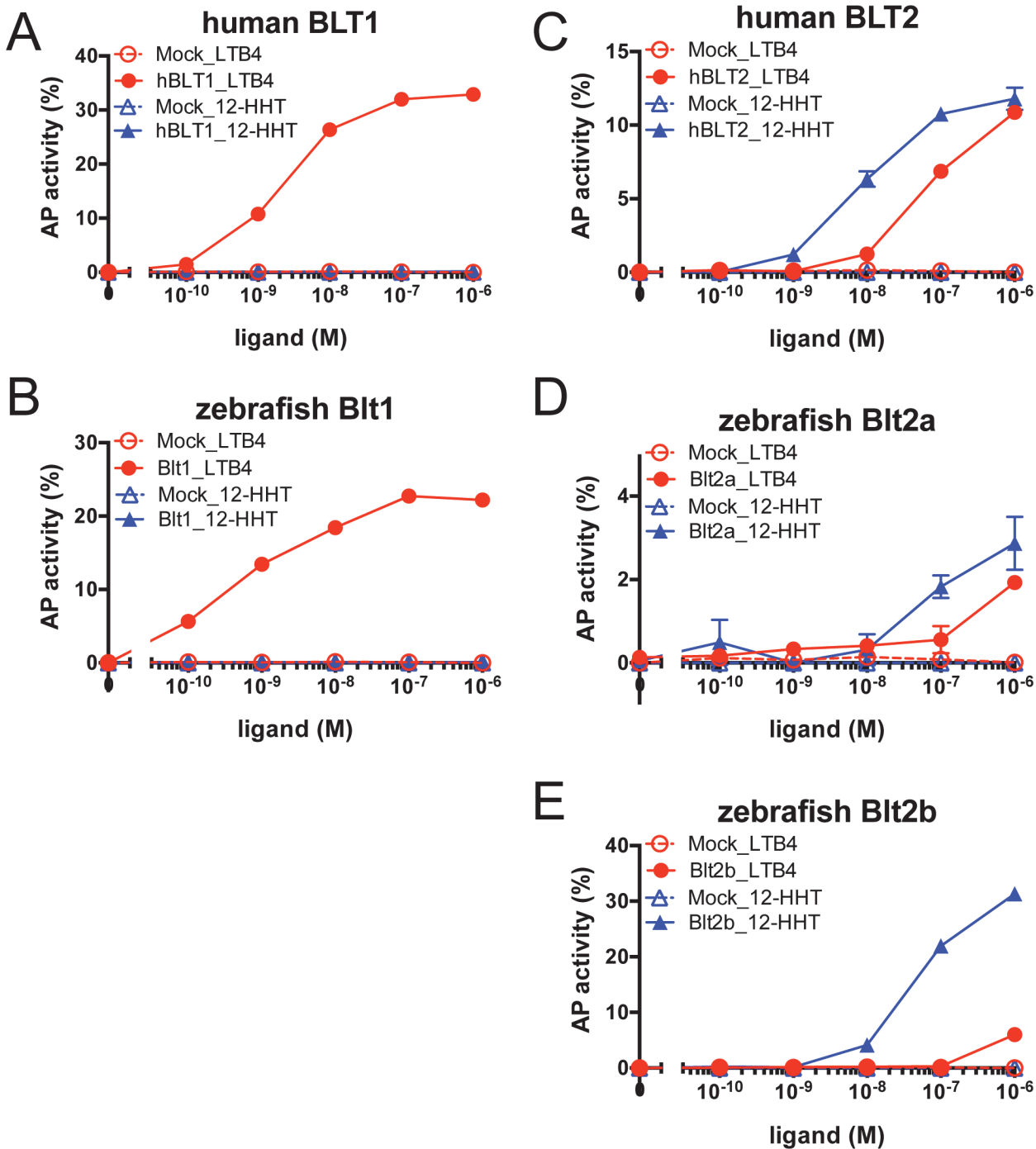


Fig 8. Ligand-dependent TGF α release via zebrafish Blt receptors. HEK293 cells expressing BLT receptors, G $\alpha_{q/11}$, and AP-TGF α were stimulated with LTB $_4$ or 12-HHT. AP-TGF α release (%) was quantified using a colorimetric AP assay using *p*-NPP as a substrate. Data are representative of at least two independent experiments with similar results.

doi:10.1371/journal.pone.0117888.g008

Expression of *blts*, *lta4h*, and *5lo* in zebrafish embryos

To confirm the gene expression of *blt1*, *blt2a*, *blt2b*, *lta4h*, and *5lo* in zebrafish embryos, reverse transcriptase (RT)-PCR was performed using mRNA of zebrafish embryos at 24 hpf. The mRNAs of *blt1*, *blt2a*, *blt2b*, *lta4h*, and *5lo* were detected in zebrafish embryos (Fig. 9A) and

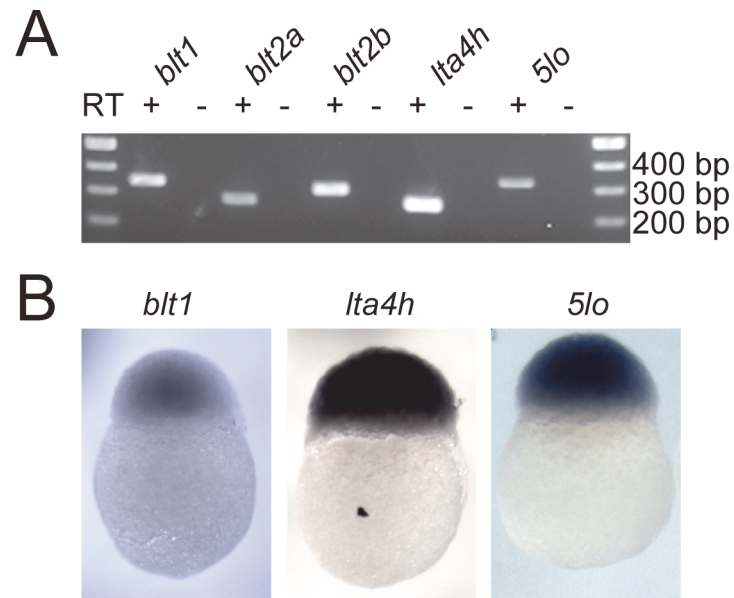


Fig 9. Expression of *blt1*, *blt2a*, *blt2b*, *lta4h*, and *5lo* in zebrafish embryos. (A) Expression of *blt1*, *blt2a*, *blt2b*, *lta4h*, and *5lo* mRNA were analyzed by RT-PCR. Total RNA was obtained from 24 hpf embryos and analyzed using specific primers for *blt1*, *blt2a*, *blt2b*, *lta4h*, and *z5lo*. (B) Expression of *blt1*, *lta4h*, and *5lo* mRNA was analyzed by whole-mount *in situ* hybridization. Zebrafish embryos (3 hpf) were hybridized with antisense probes.

doi:10.1371/journal.pone.0117888.g009

whole-mount *in situ* hybridization revealed that *blt1*, *lta4h*, and *5lo* were widely expressed at 3 hpf (Fig. 9B).

The LTB₄-BLT1 axis is required for epiboly

To investigate the roles of Blt1 in zebrafish embryogenesis, we used two *blt1* morpholino anti-sense oligonucleotides: *blt1* MO blocks the translation of mature mRNAs and *blt1* spl MO blocks the normal splicing of *blt1* (Fig. 10A). We confirmed the efficiency and specificity of the *blt1* MO using a modified EGFP construct harboring the morpholino target sequence upstream of the respective start codon (S1 Fig. A and B). To confirm the knockdown of *blt1* by the *blt1* spl MO, we performed RT-PCR analysis using primer sets that amplify normal transcripts (*blt1_fw* and *blt1_rv2*, Fig. 10A) and abnormal transcripts with un-spliced introns (*blt1_fw* and *blt1_rv*, Fig. 10A). Injection of the *blt1* spl MO dramatically reduced the correctly spliced *blt1* transcripts (Fig. 10A, middle) and increased levels of the abnormal transcripts (Fig. 10A, low). These results suggested that the *blt1* spl MO efficiently knocked down *blt1* in zebrafish. We confirmed the efficiency and specificity of an *lta4h* MO using a modified EGFP construct harboring the morpholino target sequence upstream of the respective start codon (S1 Fig. C and D).

Interestingly, injection of either the *blt1* MO, *blt1* spl MO, or *lta4h* MO, but not injection of a control MO, resulted in a severe delay in epiboly during gastrulation (Fig. 10B and 10C). These results suggest that the LTB₄-BLT1 axis is required for normal epiboly in zebrafish development.

Discussion

In this study, we identified and characterized one zebrafish BLT1-like receptor and two zebrafish BLT2-like receptors. Knockdown of *blt1* delayed epiboly at gastrulation of zebrafish

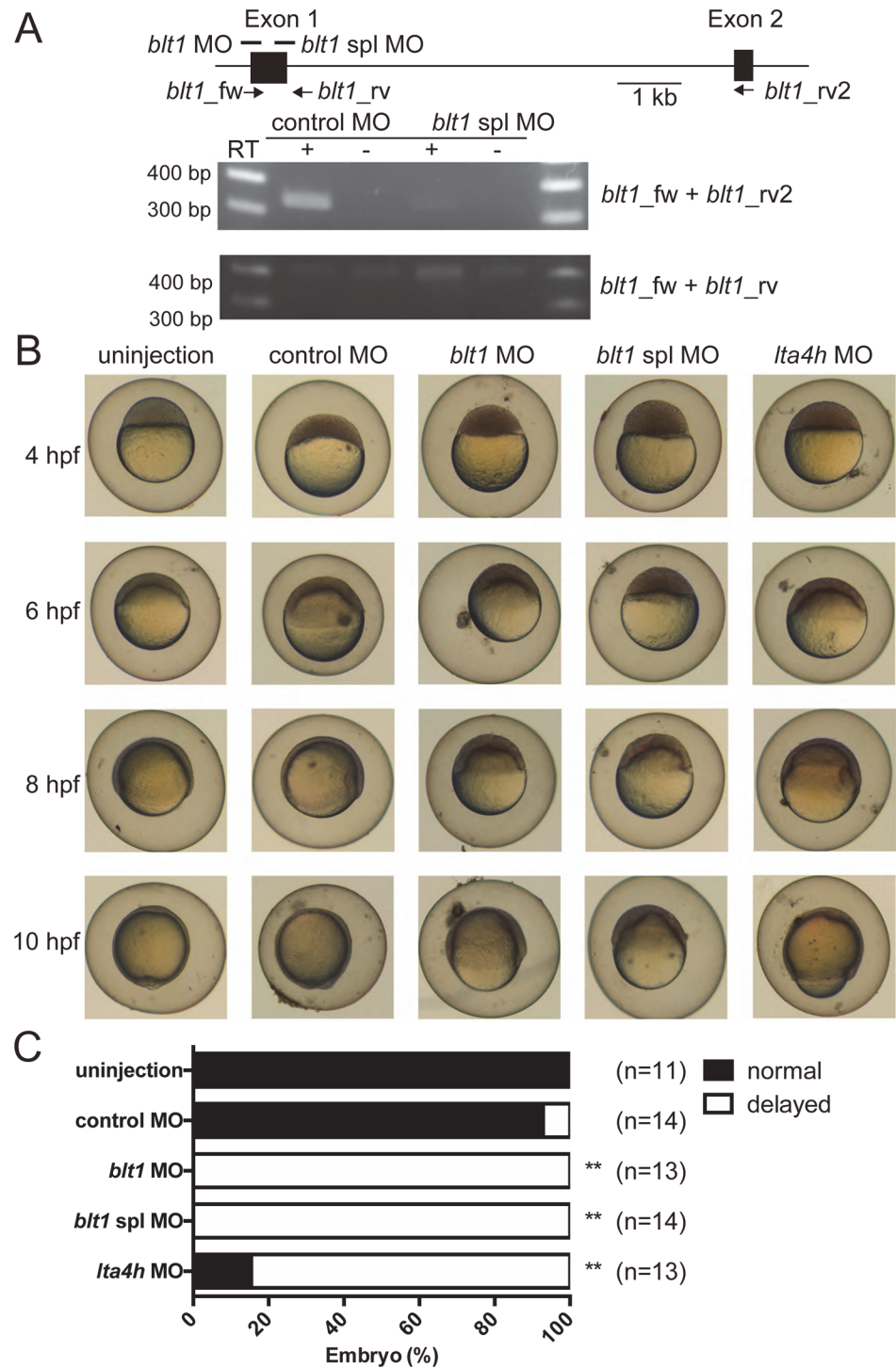


Fig 10. Morpholino-mediated knockdown of *blt1* and *lta4h* affects epiboly. (A) Diagram of a partial map of *blt1* genomic DNA. Exons and introns are shown as boxes and lines, respectively. Two nonoverlapping *blt1* MOs, *blt1* MO and *blt1 spl* MO, were designed to target translation and splicing of Blt1, respectively. The *blt1* MO should eliminate the transcription of exon 1, which contains the translation start site, resulting in aberrant protein synthesis. The efficacy of *blt1 spl* MO was validated by RT-PCR using *blt1_fw* and *blt1_rv* or *blt1_rv2*. Total RNA was isolated from *blt1 spl* MO or control MO-injected embryos at 24 hpf. Reduced expression of normal spliced *blt1* transcripts and increased mis-spliced *blt1* transcripts are shown. (B) Representative images of delayed epiboly of *blt1* and *lta4h* morphants from 4 to 10 hpf. Embryos were

injected with 2.5 ng MOs at the 1- to 2-cell stage. (C) Histogram illustrating the percentages of normal and delayed embryos. **, $P < 0.005$, one-way ANOVA with Bonferroni post-hoc test. Data are representative of at least two independent experiments with similar results.

doi:10.1371/journal.pone.0117888.g010

embryos. Database screening by sequence homology to human BLT1 and BLT2 identified three putative zebrafish Blts (Fig. 1–3) that share relatively low homologies to human and mouse BLT1 (~40%, Fig. 3A and 3B). Crystal structures of BLT1 and BLT2 have not been reported, but a structural model of the ligand binding site of BLT1 has been [26]. Alanine substitution of residues predicted to be potential ligand contact points in human BLT1, H94, Y102 (helix III), R156 (helix IV), E185 (helix V), and N241 (helix VI) resulted in reduced binding affinity, and all of these residues are conserved among zebrafish Blt1 and human and mouse BLT1 (Fig. 1). The R156A mutant of human BLT1 failed to show any [³H]LTB₄ binding; R156 is the predicted binding site for the carboxyl group of LTB₄ [26]. Among zebrafish Blt2a and Blt2b and human and mouse BLT2, all of these amino acids with the exception of H94 are conserved (Fig. 2), suggesting that H94 in helix III may be important in distinguishing between the chemical structures of LTB₄ and 12-HHT. An evolutionary tree (Fig. 3B) suggests that the gene duplication of BLT1 and BLT2 occurred after the fish branched off from the other vertebrates. The presence of two BLT2-type receptors in zebrafish suggests that BLT2 may have specific roles in zebrafish that are not required in mammals.

To identify the ligands of putative zebrafish BLTs, we constructed expression vectors for the zebrafish Blts and conducted experiments to monitor GPCR-dependent signaling (Fig. 5–8). Previously, we found that the level of BLT1 on the plasma membrane is always higher than BLT2 in various cultured cells when overexpressed under the same promoter. Both human BLT1 and zebrafish Blt1 were expressed on the cell surface at a higher level than human BLT2, or zebrafish Blt2a or Blt2b (Fig. 4). The GPCR assays conducted here all suggest that Blt1 is a zebrafish ortholog of BLT1, and that Blt2a and Blt2b are zebrafish orthologs of BLT2 (Fig. 5–8). RT-PCR and whole-mount *in situ* hybridization of zebrafish embryos showed that mRNAs of *blt1*, as well as *lta4h* and *5lo*, enzymes mediating LTB₄ production, were detected in zebrafish embryos (Fig. 9). The *blt1* and *lta4h* knockdown experiments indicated that the LTB₄-Blt1 axis is involved in epiboly at gastrulation (Fig. 10).

Gastrulation involves a series of coordinated cell movements that establish the germ layers and the major body axes of the embryos [27]. Epiboly, which involves the thinning and spreading of a multilayered cell sheet, is the first coordinated cell movement of zebrafish gastrulation and occurs after the ninth or tenth zygotic cell division. Epiboly is visualized as the thinning and spreading of the blastoderm over the yolk. Since epiboly is initiated prior to the other cell movements in zebrafish gastrulation, the initial events in gastrulation can be studied in isolation from later, more complex cell movements [28–30]. Numerous molecules are involved in epiboly including microtubules, microfilaments, cell adhesion proteins, kinases, and transcription factors [27]. The prostaglandin biosynthetic enzymes cyclooxygenase-1 (Cox-1) and prostaglandin E₂ synthase (Ptges) are also involved in epiboly. Treatment with 50 μM of indomethacin caused gastrulation arrest at 50% epiboly stage and 25 μM of indomethacin resulted in milder defect. Indomethacin-dependent epiboly defects were rescued by co-incubation with 1 μM PGE₂ [31,32].

Lin *et al.* reported that Gα_{12/13} regulates epiboly formation through two distinct mechanisms: limiting E-cadherin activity and modulating the organization of the actin cytoskeleton [33,34]. In mammals, BLT1 activates small GTPases and induces the reorganization of actin cytoskeleton [35–37]; BLT1 activates leukocyte migration and firm adhesion to endothelial cells

[10,38]. Thus, BLT1 may modulate the organization of the actin cytoskeleton and mediate cell migration in epiboly of zebrafish embryo.

We were not able to rescue the delay in epiboly by co-injection of MOs and *blt1* mRNA, suggesting that the localization and levels of Blt1 expression may be critical for proper epiboly. Although further analyses are required to understand the *in vivo* roles of Blt1 in epiboly, the molecular identification of zebrafish Blts will be useful for studying the *in vivo* roles of these receptors in zebrafish.

Supporting Information

S1 Fig. Specificity of *blt1* and *lta4h* morpholinos. (A) 5' sequence of EGFP mRNA designed to evaluate the function of the *blt1* MO. The underline indicates the *blt1* MO target sequence, the start codon is highlighted in blue, and the beginning of the open reading frame (ORF) of EGFP is highlighted in green. (B) Representative images of the effects of the *blt1* MO on the expression of control EGFP and *blt1* MO-EGFP. Translation of EGFP mRNA containing the *blt1* MO target sequence is blocked by the *blt1* MO. Control EGFP is not blocked by the *blt1* MO. Embryos were injected with a mix of mRNA (250 pg) and MO (2.5 ng) at the one cell stage. EGFP fluorescence and bright-field (BF) images were taken at 7 hpf. (C) 5' sequence of EGFP mRNA designed to evaluate the function of the *lta4h* MO. The underline indicates the *lta4h* MO target sequence, the start codon is highlighted in blue, and the beginning of the ORF of EGFP is highlighted in green. (D) Representative images of the effects of the *lta4h* MO on the expression of the *lta4h* MO-EGFP. Translation of EGFP mRNA containing the *lta4h* MO target sequence is blocked by the *lta4h* MO but not by a control MO. Embryos were injected with a mix of mRNA (250 pg) and MO (2.5 ng) at the one cell stage. EGFP fluorescence and BF images were taken at 6.5 hpf. (TIF)

Acknowledgments

We thank Dr. Hiroyuki Toh (CBRC, AIST) for valuable advice on searching for the zebrafish BLTs and Dr. Atsuo Kawahara (University of Yamanashi) for useful suggestions. We appreciate the technical support provided by the Research Support Center, Graduate School of Medical Sciences, Kyushu University.

Author Contributions

Conceived and designed the experiments: TO TI TY. Performed the experiments: TO TI. Analyzed the data: TO TI. Wrote the paper: TO TI TY.

References

1. Samuelsson B, Dahlen SE, Lindgren JA, Rouzer CA, Serhan CN (1987) Leukotrienes and lipoxins: structures, biosynthesis, and biological effects. *Science* 237: 1171–1176. PMID: [2820055](#)
2. Okuno T, Yokomizo T, Hori T, Miyano M, Shimizu T (2005) Leukotriene B4 receptor and the function of its helix 8. *J Biol Chem* 280: 32049–32052. PMID: [16046389](#)
3. Yokomizo T, Izumi T, Chang K, Takuwa Y, Shimizu T (1997) A G-protein-coupled receptor for leukotriene B4 that mediates chemotaxis. *Nature* 387: 620–624. PMID: [9177352](#)
4. Yokomizo T, Kato K, Terawaki K, Izumi T, Shimizu T (2000) A second leukotriene B(4) receptor, BLT2. A new therapeutic target in inflammation and immunological disorders. *J Exp Med* 192: 421–432. PMID: [10934230](#)
5. Okuno T, Iizuka Y, Okazaki H, Yokomizo T, Taguchi R, et al. (2008) 12(S)-Hydroxyheptadeca-5Z, 8E, 10E-trienoic acid is a natural ligand for leukotriene B4 receptor 2. *The Journal of experimental medicine* 205: 759–766. doi: [10.1084/jem.20072329](#) PMID: [18378794](#)

6. Matsunobu T, Okuno T, Yokoyama C, Yokomizo T (2013) Thromboxane A synthase-independent production of 12-hydroxyheptadecatrienoic acid, a BLT2 ligand. *J Lipid Res* 54: 2979–2987. doi: [10.1194/jlr.M037754](https://doi.org/10.1194/jlr.M037754) PMID: [24009185](https://pubmed.ncbi.nlm.nih.gov/24009185/)
7. Huang WW, Garcia-Zepeda EA, Sauty A, Oettgen HC, Rothenberg ME, et al. (1998) Molecular and biological characterization of the murine leukotriene B4 receptor expressed on eosinophils. *J Exp Med* 188: 1063–1074. PMID: [9743525](https://pubmed.ncbi.nlm.nih.gov/9743525/)
8. Miyahara N, Ohnishi H, Matsuda H, Miyahara S, Takeda K, et al. (2008) Leukotriene B4 receptor 1 expression on dendritic cells is required for the development of Th2 responses and allergen-induced airway hyperresponsiveness. *J Immunol* 181: 1170–1178. PMID: [18606670](https://pubmed.ncbi.nlm.nih.gov/18606670/)
9. Toda A, Terawaki K, Yamazaki S, Saeki K, Shimizu T, et al. (2010) Attenuated Th1 induction by dendritic cells from mice deficient in the leukotriene B4 receptor 1. *Biochimie* 92: 682–691. doi: [10.1016/j.biochi.2009.12.002](https://doi.org/10.1016/j.biochi.2009.12.002) PMID: [20004699](https://pubmed.ncbi.nlm.nih.gov/20004699/)
10. Tager AM, Bromley SK, Medoff BD, Islam SA, Bercury SD, et al. (2003) Leukotriene B4 receptor BLT1 mediates early effector T cell recruitment. *Nat Immunol* 4: 982–990. PMID: [12949531](https://pubmed.ncbi.nlm.nih.gov/12949531/)
11. Hikiji H, Ishii S, Yokomizo T, Takato T, Shimizu T (2009) A distinctive role of the leukotriene B4 receptor BLT1 in osteoclastic activity during bone loss. *Proc Natl Acad Sci U S A* 106: 21294–21299. doi: [10.1073/pnas.0905209106](https://doi.org/10.1073/pnas.0905209106) PMID: [19965376](https://pubmed.ncbi.nlm.nih.gov/19965376/)
12. Back M, Dahlen SE, Drazen JM, Evans JF, Serhan CN, et al. (2011) International Union of Basic and Clinical Pharmacology. LXXXIV: leukotriene receptor nomenclature, distribution, and pathophysiological functions. *Pharmacol Rev* 63: 539–584. doi: [10.1124/pr.110.004184](https://doi.org/10.1124/pr.110.004184) PMID: [21771892](https://pubmed.ncbi.nlm.nih.gov/21771892/)
13. Iizuka Y, Okuno T, Saeki K, Uozaki H, Okada S, et al. (2010) Protective role of the leukotriene B4 receptor BLT2 in murine inflammatory colitis. *FASEB journal: official publication of the Federation of American Societies for Experimental Biology* 24: 4678–4690. doi: [10.1096/fj.10-165050](https://doi.org/10.1096/fj.10-165050) PMID: [20667973](https://pubmed.ncbi.nlm.nih.gov/20667973/)
14. Matsunaga Y, Fukuyama S, Okuno T, Sasaki F, Matsunobu T, et al. (2013) Leukotriene B4 receptor BLT2 negatively regulates allergic airway eosinophilia. *FASEB J* 27: 3306–3314. doi: [10.1096/fj.12-217000](https://doi.org/10.1096/fj.12-217000) PMID: [23603839](https://pubmed.ncbi.nlm.nih.gov/23603839/)
15. Liu M, Saeki K, Matsunobu T, Okuno T, Koga T, et al. (2014) 12-Hydroxyheptadecatrienoic acid promotes epidermal wound healing by accelerating keratinocyte migration via the BLT2 receptor. *J Exp Med* 211: 1063–1078. doi: [10.1084/jem.20132063](https://doi.org/10.1084/jem.20132063) PMID: [24821912](https://pubmed.ncbi.nlm.nih.gov/24821912/)
16. Kimmel CB, Ballard WW, Kimmel SR, Ullmann B, Schilling TF (1995) Stages of embryonic development of the zebrafish. *Dev Dyn* 203: 253–310. PMID: [8589427](https://pubmed.ncbi.nlm.nih.gov/8589427/)
17. Meijer AH, Spaink HP (2011) Host-pathogen interactions made transparent with the zebrafish model. *Curr Drug Targets* 12: 1000–1017. PMID: [21366518](https://pubmed.ncbi.nlm.nih.gov/21366518/)
18. Bischel LL, Mader BR, Green JM, Huttenlocher A, Beebe DJ (2013) Zebrafish Entrapment By Restriction Array (ZEBRA) device: a low-cost, agarose-free zebrafish mounting technique for automated imaging. *Lab Chip* 13: 1732–1736. doi: [10.1039/c3lc50099c](https://doi.org/10.1039/c3lc50099c) PMID: [23503983](https://pubmed.ncbi.nlm.nih.gov/23503983/)
19. Tobin DM, Vary JC Jr., Ray JP, Walsh GS, Dunstan SJ, et al. (2010) The ItA4h locus modulates susceptibility to mycobacterial infection in zebrafish and humans. *Cell* 140: 717–730. doi: [10.1016/j.cell.2010.02.013](https://doi.org/10.1016/j.cell.2010.02.013) PMID: [20211140](https://pubmed.ncbi.nlm.nih.gov/20211140/)
20. Tobin DM, Roca FJ, Oh SF, McFarland R, Vickery TW, et al. (2012) Host genotype-specific therapies can optimize the inflammatory response to mycobacterial infections. *Cell* 148: 434–446. doi: [10.1016/j.cell.2011.12.023](https://doi.org/10.1016/j.cell.2011.12.023) PMID: [22304914](https://pubmed.ncbi.nlm.nih.gov/22304914/)
21. Niwa H, Yamamura K, Miyazaki J (1991) Efficient selection for high-expression transfectants with a novel eukaryotic vector. *Gene* 108: 193–199. PMID: [1660837](https://pubmed.ncbi.nlm.nih.gov/1660837/)
22. Inoue A, Ishiguro J, Kitamura H, Arima N, Okutani M, et al. (2012) TGFalpha shedding assay: an accurate and versatile method for detecting GPCR activation. *Nat Methods* 9: 1021–1029. doi: [10.1038/nmeth.2172](https://doi.org/10.1038/nmeth.2172) PMID: [22983457](https://pubmed.ncbi.nlm.nih.gov/22983457/)
23. Okuno T, Ago H, Terawaki K, Miyano M, Shimizu T, et al. (2003) Helix 8 of the leukotriene B4 receptor is required for the conformational change to the low affinity state after G-protein activation. *J Biol Chem* 278: 41500–41509. PMID: [12902330](https://pubmed.ncbi.nlm.nih.gov/12902330/)
24. Kuniyeda K, Okuno T, Terawaki K, Miyano M, Yokomizo T, et al. (2007) Identification of the intracellular region of the leukotriene B4 receptor type 1 that is specifically involved in Gi activation. *J Biol Chem* 282: 3998–4006. PMID: [17158791](https://pubmed.ncbi.nlm.nih.gov/17158791/)
25. Yasuda D, Okuno T, Yokomizo T, Hori T, Hirota N, et al. (2009) Helix 8 of leukotriene B4 type-2 receptor is required for the folding to pass the quality control in the endoplasmic reticulum. *FASEB J* 23: 1470–1481. doi: [10.1096/fj.08-125385](https://doi.org/10.1096/fj.08-125385) PMID: [19126593](https://pubmed.ncbi.nlm.nih.gov/19126593/)
26. Basu S, Jala VR, Mathis S, Rajagopal ST, Del Prete A, et al. (2007) Critical role for polar residues in coupling leukotriene B4 binding to signal transduction in BLT1. *J Biol Chem* 282: 10005–10017. PMID: [17237498](https://pubmed.ncbi.nlm.nih.gov/17237498/)

27. Lepage SE, Bruce AE (2010) Zebrafish epiboly: mechanics and mechanisms. *Int J Dev Biol* 54: 1213–1228. doi: [10.1387/ijdb.093028sl](https://doi.org/10.1387/ijdb.093028sl) PMID: [20712002](https://pubmed.ncbi.nlm.nih.gov/20712002/)
28. Warga RM, Kimmel CB (1990) Cell movements during epiboly and gastrulation in zebrafish. *Development* 108: 569–580. PMID: [2387236](https://pubmed.ncbi.nlm.nih.gov/2387236/)
29. Rohde LA, Heisenberg CP (2007) Zebrafish gastrulation: cell movements, signals, and mechanisms. *Int Rev Cytol* 261: 159–192. PMID: [17560282](https://pubmed.ncbi.nlm.nih.gov/17560282/)
30. Solnica-Krezel L, Sepich DS (2012) Gastrulation: making and shaping germ layers. *Annu Rev Cell Dev Biol* 28: 687–717. doi: [10.1146/annurev-cellbio-092910-154043](https://doi.org/10.1146/annurev-cellbio-092910-154043) PMID: [22804578](https://pubmed.ncbi.nlm.nih.gov/22804578/)
31. Cha YI, Kim SH, Solnica-Krezel L, Dubois RN (2005) Cyclooxygenase-1 signaling is required for vascular tube formation during development. *Dev Biol* 282: 274–283. PMID: [15936346](https://pubmed.ncbi.nlm.nih.gov/15936346/)
32. Cha YI, Kim SH, Sepich D, Buchanan FG, Solnica-Krezel L, et al. (2006) Cyclooxygenase-1-derived PGE2 promotes cell motility via the G-protein-coupled EP4 receptor during vertebrate gastrulation. *Genes Dev* 20: 77–86. PMID: [16391234](https://pubmed.ncbi.nlm.nih.gov/16391234/)
33. Lin F, Sepich DS, Chen S, Topczewski J, Yin C, et al. (2005) Essential roles of G α 12/13 signaling in distinct cell behaviors driving zebrafish convergence and extension gastrulation movements. *J Cell Biol* 169: 777–787. PMID: [15928205](https://pubmed.ncbi.nlm.nih.gov/15928205/)
34. Lin F, Chen S, Sepich DS, Panizzi JR, Clendenon SG, et al. (2009) G α 12/13 regulate epiboly by inhibiting E-cadherin activity and modulating the actin cytoskeleton. *J Cell Biol* 184: 909–921. doi: [10.1083/jcb.200805148](https://doi.org/10.1083/jcb.200805148) PMID: [19307601](https://pubmed.ncbi.nlm.nih.gov/19307601/)
35. Kavelaars A, Vroon A, Raatgever RP, Fong AM, Premont RT, et al. (2003) Increased acute inflammation, leukotriene B4-induced chemotaxis, and signaling in mice deficient for G protein-coupled receptor kinase 6. *J Immunol* 171: 6128–6134. PMID: [14634128](https://pubmed.ncbi.nlm.nih.gov/14634128/)
36. Costa MF, de Souza-Martins R, de Souza MC, Benjamim CF, Piva B, et al. (2010) Leukotriene B4 mediates gammadelta T lymphocyte migration in response to diverse stimuli. *J Leukoc Biol* 87: 323–332. doi: [10.1189/jlb.0809563](https://doi.org/10.1189/jlb.0809563) PMID: [19880577](https://pubmed.ncbi.nlm.nih.gov/19880577/)
37. Moraes J, Assreuy J, Canetti C, Barja-Fidalgo C (2010) Leukotriene B4 mediates vascular smooth muscle cell migration through α v β 3 integrin transactivation. *Atherosclerosis* 212: 406–413. doi: [10.1016/j.atherosclerosis.2010.06.009](https://doi.org/10.1016/j.atherosclerosis.2010.06.009) PMID: [20580365](https://pubmed.ncbi.nlm.nih.gov/20580365/)
38. Johansson AS, Haeggstrom JZ, Palmblad J (2011) Commonly used leukotriene B4 receptor antagonists possess intrinsic activity as agonists in human endothelial cells: Effects on calcium transients, adhesive events and mediator release. *Prostaglandins Leukot Essent Fatty Acids* 84: 109–112. doi: [10.1016/j.plefa.2010.11.003](https://doi.org/10.1016/j.plefa.2010.11.003) PMID: [21183325](https://pubmed.ncbi.nlm.nih.gov/21183325/)